

At14a-Like1 participates in membrane-associated mechanisms promoting growth during drought in *Arabidopsis thaliana*

M. Nagaraj Kumar¹, Yi-Fang Hsieh¹, and Paul E. Verslues²

Institute of Plant and Microbial Biology, Academia Sinica, Taipei, Taiwan 115

Edited by Natasha V. Raikhel, Center for Plant Cell Biology, Riverside, CA, and approved July 10, 2015 (received for review May 27, 2015)

Limited knowledge of how plants regulate their growth and metabolism in response to drought and reduced soil water potential has impeded efforts to improve stress tolerance. Increased expression of the membrane-associated protein At14a-like1 (AFL1) led to increased growth and accumulation of the osmoprotective solute proline without negative effects on unstressed plants. Conversely, inducible RNA-interference suppression of AFL1 decreased growth and proline accumulation during low water potential while having no effect on unstressed plants. AFL1 overexpression lines had reduced expression of many stress-responsive genes, suggesting AFL1 may promote growth in part by suppression of negative regulatory genes. AFL1 interacted with the endomembrane proteins protein disulfide isomerase 5 (PDI5) and NAI2, with the PDI5 interaction being particularly increased by stress. PDI5 and NAI2 are negative regulatory factors, as *pdi5*, *nai2*, and *pdi5-2nai2-3* mutants had increased growth and proline accumulation at low water potential. AFL1 also interacted with Adaptor protein2-2A (AP2-2A), which is part of a complex that recruits cargo proteins and promotes assembly of clathrin-coated vesicles. AFL1 colocalization with clathrin light chain along the plasma membrane, together with predictions of AFL1 structure, were consistent with a role in vesicle formation or trafficking. Fractionation experiments indicated that AFL1 is a peripheral membrane protein associated with both plasma membrane and endomembranes. These data identify classes of proteins (AFL1, PDI5, and NAI2) not previously known to be involved in drought signaling. AFL1-predicted structure, protein interactions, and localization all indicate its involvement in previously uncharacterized membrane-associated drought sensing or signaling mechanisms.

drought | At14a | vesicle endocytosis | protein disulfide isomerase | clathrin adaptor AP2-2a

Even relatively mild drought that causes reduced soil water potential (ψ_w) can result in dramatically reduced plant growth and agricultural productivity. Physiological analyses have shown that plant growth is actively down-regulated during drought and is not limited by carbon supply (1–3). Reductions of growth help ensure survival by conserving water but can be undesirable for agriculture, as plant productivity is reduced more than need be if growth were less sensitive to changes in water status (3). Also, specific metabolic pathways, such as proline metabolism, are stress regulated and contribute to drought tolerance.

The sensing and signaling mechanisms controlling growth and metabolic responses to drought remain unclear. Many hypotheses of how plants sense water loss center on detection of mechanical stimuli generated by loss of turgor and cell shrinkage. This includes changes in membrane shape or disruption of cell wall–cell membrane connections possibly detected by proteins, such as mechanosensitive channels or receptor-like kinases that bind cell wall components (4–9). Proteins that induce or detect membrane curvature are known in mammalian cells (10) but have been little considered in plants. Also, in analogy to mammalian cells, integrin-related proteins have been hypothesized to play stress-sensing roles in plant cells. Plants lack clear orthologs

to integrins. Nonetheless, modeling has identified at least one *Arabidopsis* protein with integrin-like structure and possible stress-related function (11), and other proteins with small integrin similarity domains also have been identified (12). Endomembrane compartments, particularly the endoplasmic reticulum (ER), are involved in responding to cytotoxic stresses such as the accumulation of unfolded proteins (13). How endomembrane proteins may be involved in responding to water limitation, and whether this may occur via mechanisms other than the unfolded protein response, is less understood. Trafficking of membrane proteins between cellular compartments is also emerging as an important aspect of plant signaling, with plasma membrane (PM) aquaporins being one example of intracellular trafficking affecting drought resistance (14). Sites of ER–PM contact have also been proposed to be critical for mechanosensing and stress tolerance (15).

With the motivation of testing a different class of protein that could have roles in sensing or signaling abiotic stress, we investigated the function of At14a-Like1 (AFL1, *At3g28270*). At14a (*At3g28300*) was first identified by immunoscreening an *Arabidopsis* expression library with antisera recognizing mammalian β_1 -integrin and was reported to be a PM-associated protein (12). A cluster of At14a-related genes, including AFL1, is present in *Arabidopsis*. AFL1 contains a small domain with similarity to integrins (domain of unknown function 677), but there is little other information that could reveal its cellular function. Our

Significance

Drought is a major cause of lost agricultural productivity. Even moderate water limitation can lead to down-regulation of plant growth; however, the underlying mechanisms of stress sensing and growth regulation are little understood. We identified At14a-Like1 (AFL1) and its interacting proteins protein disulfide isomerase 5 (PDI5) and NAI2 as positive and negative regulators, respectively, of growth and proline accumulation. Despite numerous ideas that membrane-based mechanisms are important for drought sensing and initial signaling, AFL1 is one of only a few membrane proteins with a demonstrated effect on drought resistance. AFL1 structure, localization, and interaction with endomembrane proteins indicate novel functions in drought signaling. Increased growth of AFL1 overexpression in plants under stress without negative effects on unstressed plants make AFL1 an attractive target for biotechnology.

Author contributions: P.E.V. designed research; M.N.K. and Y.-F.H. performed research; M.N.K., Y.-F.H., and P.E.V. analyzed data; and P.E.V. wrote the paper.

The authors declare no conflict of interest.

This article is a PNAS Direct Submission.

Data deposition: The data reported in this paper have been deposited in the Gene Expression Omnibus (GEO) database, www.ncbi.nlm.nih.gov/geo (accession no. GSE62413).

¹M.N.K. and Y.-F.H. contributed equally to this work.

²To whom correspondence should be addressed. Email: paulv@gate.sinica.edu.tw.

This article contains supporting information online at www.pnas.org/lookup/suppl/doi:10.1073/pnas.1510140112/-DCSupplemental.

investigation found that AFL1 has a dramatic effect on plant growth during drought and identified AFL1 association with endomembrane proteins and clathrin-coated vesicle formation at the PM as key aspects of AFL1 cellular function.

Results

AFL1 Promotes Growth and Proline Accumulation and Alters the Stress-Responsive Transcriptome. Although AFL1 contains a small integrin-similarity domain, the overall structure was clearly different from integrins (*SI Appendix, Fig. S1A*, see following text). This structure was intriguing, as we know little of membrane-associated proteins involved in abiotic stress. In previous microarray experiments, AFL1 gene expression was induced 30-fold by exposure to low ψ_w for 96 h (16). RT-PCR verified a strong induction of AFL1 expression (*SI Appendix, Fig. S1B*), and a stress-increased protein of appropriate size was detected using a commercial antibody recognizing β_1 -integrin (*SI Appendix, Fig. S1C*). Antisera specifically recognizing the N-terminal domain of AFL1 confirmed that AFL1 protein abundance was dramatically increased by low ψ_w (*SI Appendix, Fig. S1D*).

To test the function of AFL1, we generated transgenic lines with 35S promoter-driven ectopic expression of AFL1 fused to either an N-terminal enhanced yellow fluorescent protein (eYFP) or a C-terminal FLAG tag (hereafter referred to as overexpression lines; AFL1 O.E. lines). Both types of AFL1 O.E. lines had essentially identical phenotypes, and combined data from both are shown in subsequent figures. Transgenic lines with dexamethasone (DEX)-inducible RNAi knockdown of AFL1 (AFL1 K.D. lines) were also generated. Quantitative RT-PCR and immunoblotting verified increased or decreased AFL1 expression in the O.E. and K.D. lines, respectively (*SI Appendix, Fig. S2*). There are no publicly available transfer-DNA mutants for AFL1.

When seedlings were transferred to either a moderate (−0.7 MPa) or more severe (−1.2 MPa) low ψ_w stress, AFL1 O.E. lines had dramatically increased (more than 60%) root elongation, increased seedling dry weight (Fig. 1A), and increased fresh weight (*SI Appendix, Fig. S3A*). The plants were also visually larger than wild-type (Fig. 1B). AFL1 overexpression had no apparent negative effect, and even increased growth, in the absence of stress (Fig. 1A). Similar results of increased rosette weight and size were seen in AFL1 O.E. plants subjected to controlled soil drying (Fig. 1C and *SI Appendix, Fig. S4*). Conversely, growth of AFL1 K.D. lines at low ψ_w was decreased by more than 40% after the addition of DEX to activate RNAi suppression of AFL1 (Fig. 1A and *SI Appendix, Fig. S3B*). RNAi suppression of AFL1 had no effect on growth in the control (Fig. 1A and *SI Appendix, Fig. S3B*), and addition of DEX had no effect on an empty vector control line (*SI Appendix, Fig. S3C*). AFL1 O.E. lines also had higher accumulation of the osmoprotective solute proline, whereas AFL1 K.D. lines had reduced proline across a range of low ψ_w severities (Fig. 1D).

AFL1 O.E. also modified the transcriptional response to low ψ_w , which in wild-type included both up- and down-regulation of many genes (*Dataset S1*). The predominant effect of AFL1 O.E. lines was to suppress gene expression: 525 genes were down-regulated by AFL1 O.E. lines in control (*Dataset S1*), and 722 genes at low ψ_w (*Dataset S1*), compared with 172 genes up-regulated by AFL1 O.E. lines in control (*Dataset S1*) and 398 at low ψ_w (*Dataset S1*). Many of these were genes already stress down-regulated in wild-type (Fig. 1E). Expression of several genes down-regulated in AFL1 O.E. lines was verified by quantitative RT-PCR (*SI Appendix, Fig. S5*). Gene ontology terms enriched in the AFL1 down-regulated genes include transcription factors, cell wall, defense response, oxidative metabolism, and membrane/endomembrane proteins (*Dataset S1*). Gene ontology terms enriched in genes up-regulated by AFL1 overexpression include protein disulfide oxidoreductase activity and redox-related metabolism, lipid metabolism, and cytokinin metabolism (*Dataset S1*). Interestingly, we found that AFL1

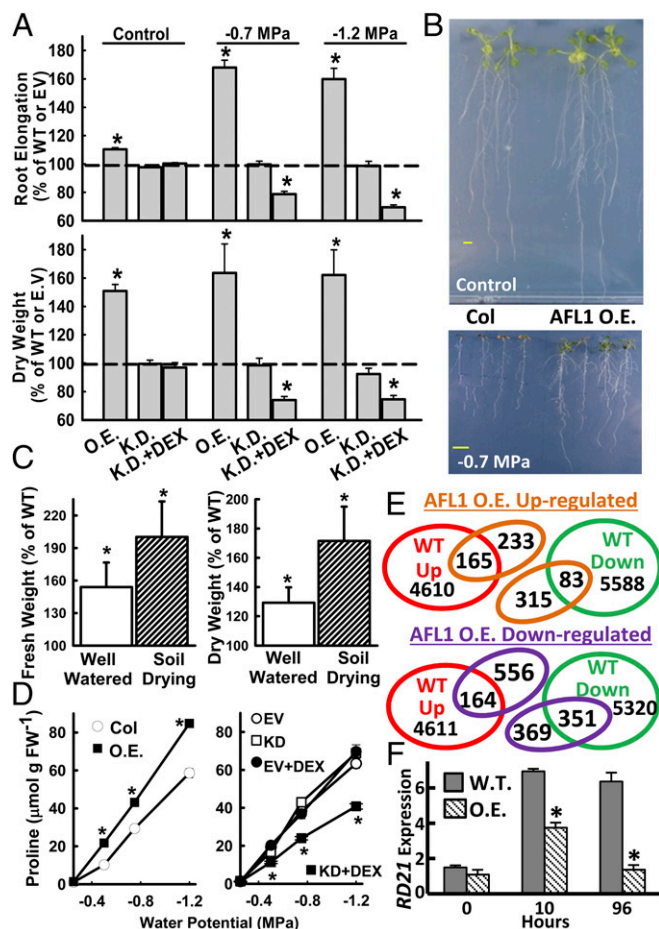


Fig. 1. AFL1 promotes growth and alters the stress transcriptome. (A) Root elongation and dry weight of AFL1 O.E. and RNAi K.D. plants after transfer to unstressed control media (−0.25 MPa) or two low ψ_w stress severities (−0.7 and −1.2 MPa). Data are means \pm SE ($n = 12$ from two independent experiments). EV, empty vector control for the K.D. lines; DEX, dexamethasone; WT, wild-type (Columbia-0). Significant differences compared with WT are indicated by * ($P \leq 0.05$). (B) Representative seedlings of WT and AFL1 O.E. 10 d after transfer to the respective treatments. (Scale bars, 1 cm.) (C) Rosette fresh weight and dry weight of AFL1 O.E. plants relative to WT in well-watered or controlled soil drying treatments. Data are means \pm SE ($n = 10$ –12 from three independent experiments). Significant differences compared with WT are indicated by * ($P \leq 0.05$). (D) Proline accumulation of AFL1 O.E. and K.D. lines across a range of low ψ_w severities (means \pm SE, $n = 12$ –36, combined from two independent experiments; significant differences marked by *). (E) Microarray gene expression profiles of WT and AFL1 O.E. (35S:YFP-AFL1) analyzed to determine whether increased AFL1 enhanced or antagonized the WT transcriptional response to low ψ_w . Full microarray results are shown in *Dataset S1*. (F) Quantitative RT-PCR analysis of *RD21*. Data are means \pm SE ($n = 4$) from two independent experiments. Significant differences ($P \leq 0.05$) relative to WT are indicated (*).

O.E. lines blocked stress induction of *RD21* (Fig. 1F), a procell death protease, the trafficking and activity of which are regulated by protein disulfide isomerase 5 (PDI5) (17). Overall, the growth and proline data indicated a key role of AFL1 in drought resistance, whereas the gene expression data raised the possibility that AFL1 may restrict the expression of genes that suppress growth during low ψ_w stress.

AFL1 Interacts with Endomembrane Proteins PDI5 and NAI2, which Act as Negative Regulators of Growth and Proline Accumulation. To understand AFL1 function, we identified interacting proteins using several methods (*SI Appendix, Fig. S6*). Yeast two-hybrid

library screening using the N-terminal domain of AFL1 as bait identified the ER chaperone PDI5 (17), the ER body protein NAI2 (18), and the NAI2-related protein TSK-associating1 (TSA1), as well as partial clones containing the C-terminal domain of AFL1 and At14a. PDI5 and NAI2 were also identified in AFL1 immunoprecipitates (Dataset S1). Additional putative AFL1-interacting proteins were identified by immunoprecipitation including AP2-2a, part of a protein complex involved in clathrin-coated vesicle formation (19), as well as other vesicle transport components and cytoskeleton-related proteins (Dataset S1).

Mating-based split-ubiquitin (mbSUS) assays using full-length AFL1 as bait confirmed interaction with PDI5, NAI2, TSA1, and AP2-2a (Fig. 2A). Also consistent with the yeast two-hybrid screening, AFL1 strongly interacted with itself. Dynamin (DRP1A) and the ER protein HAP6 were identified in AFL1 immunoprecipitates but did not interact with AFL1 in mbSUS. Possibly, DRP1A and HAP6 indirectly associate with AFL1 via larger protein complexes (or were nonspecific contaminants of the immunoprecipitates).

AFL1 interactions were assayed in planta, using ratiometric bimolecular fluorescence complementation (rBiFC), which allows the BiFC signal to be normalized relative to a constitutively expressed RFP reporter (20). Assays were conducted by transient expression in intact seedlings (21). Interestingly, AFL1 interaction with itself, PDI5, and NAI2 was promoted 8–16-fold by low ψ_w (Fig. 2B and C). Western blotting of seedlings after rBiFC assay showed that the stimulated interaction of AFL1 and PDI5 in the stress treatment was unlikely to be explained by differences in protein expression (Fig. 2D). Coimmunoprecipitation also consistently found more PDI5-AFL1 association after low ψ_w stress treatment (Fig. 2E).

For AFL1 interaction with NAI2, the increased rBiFC signal in the low ψ_w treatment could have been caused either by difference in protein expression or increased interaction (Fig. 2D). The Western blot result must be interpreted with some caution, as it reflects both the number of cells expressing the BiFC constructs and the expression level in those cells. TSA1 had a very limited rBiFC interaction with AFL1, which was not stimulated by stress (Fig. 2C and D). Thus, TSA1 may not function with AFL1 in vivo. Consistent with the mbSUS assays, no AFL1-HAP6 interaction was observed in rBiFC.

Low ψ_w stimulation of AFL1-NAI2 and AFL1-PDI5 interactions could also be detected using another vector system (SI Appendix, Fig. S7A). In contrast to the PDI5-AFL1 interaction, the previously reported interaction of PDI5 with RD21 (17) could be readily detected under both control and stress conditions (SI Appendix, Fig. S7B). AFL1-PDI5 rBiFC with coexpression of an ER marker (22) showed extensive, but not complete, overlap of the signals (SI Appendix, Fig. S8A). Thus, AFL1-PDI5 interaction is likely to occur in the endomembrane system, but perhaps not exclusively in the ER. In leaf epidermal cells, AFL1 was found in tubule-like structures typical of ER (SI Appendix, Fig. S8B).

The interaction experiments suggested that PDI5 and NAI2 may function with AFL1 in stress signaling occurring in the endomembrane system. Consistent with this, *pdi5* and *nai2* mutants (SI Appendix, Fig. S9) had increased root elongation, dry weight, and proline (Fig. 2F and G), with the only exception being that the effect of *NAI2* was specific to the shoot. A *pdi5-2nai2-3* double mutant had an even greater increase in seedling

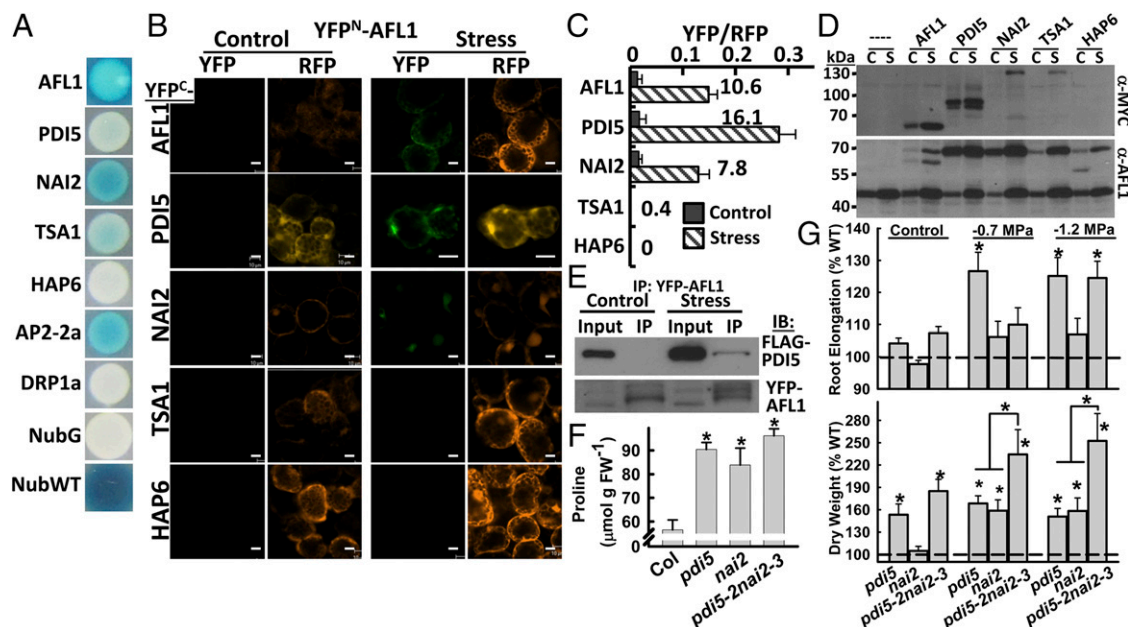


Fig. 2. AFL1 has stress-enhanced interaction with ER signaling proteins PDI5 and NAI2, which act as negative regulators of growth and proline. (A) mbSUS protein interaction assays. NubG is a negative control, and NubWT is a positive control. No interaction was detected for HAP6 and DRP1A. (B) rBiFC of AFL1 and putative interactors in control or stress (−1.2 MPa, 24 h) treated seedlings. YFP is the BiFC signal. RFP is a constitutively expressed reporter used to normalize BiFC fluorescence. Leaf mesophyll cells are shown. (Scale bars, 20 μm.) (C) Relative BiFC signal for AFL1 interactions. Numbers by the bars indicate the fold increase of YFP/RFP ratio in stress versus control for each interaction. Data are \pm SE ($n = 6-11$). (D) Immunoblot of samples collected after rBiFC assay. Anti-MYC was used to detect the YFP^C-protein fusions, whereas AFL1-specific antisera were used to detect the YFP^N-AFL1 fusion proteins. In the AFL1 blot, both native AFL1 (47 kDa) and the AFL1 fusion protein (70 kDa) can be seen. C, unstressed control; S, low ψ_w stress treated. (E) Co-immunoprecipitation (Co-IP) of PDI5-FLAG with YFP-AFL1 in control and stress treated seedlings. Three independent Co-IP experiments gave consistent results. (F) Proline accumulation of WT (Col), *pdi5* (combined data of *pdi5-1* and *pdi5-2*), *nai2* (combined data of *nai2-1* and *nai2-3*), and *pdi5-2nai2-3* at 96 h after transfer to −1.2 MPa. Data are means \pm SE ($n = 6-12$ from two independent experiments). Significant differences compared with wild-type are indicated by * ($P \leq 0.05$). (G) Root elongation and seedling dry weight for *pdi5* (*pdi5-1* and *pdi5-2*), *nai2* (*nai2-1* and *nai2-3*), and *pdi5-2nai2-3* under control condition or two low ψ_w severities (−0.7 and −1.2 MPa). Data are means \pm SE [$n = 6-9$ (fresh and dry weight) or 12–18 (root elongation) from three independent experiments]. Significant differences compared with wild-type or between the single versus the double mutant are indicated by * ($P \leq 0.05$).

dry weight (up to 200% of wild-type) after low ψ_w treatment, whereas proline accumulation did not increase further, and root elongation had only the *pdi5* effect (Fig. 2 *F* and *G*). These data indicated that PDI5 and NAI2 have partially overlapping roles as negative regulators of growth and proline accumulation at low ψ_w .

AFL1 Colocalization with Clathrin Light Chain as Well as Structural Modeling Indicate an Association of AFL1 with Clathrin-Coated Vesicle Assembly at the Plasma Membrane. Previous reports on At14a described it as a PM protein (12, 23, 24), and AFL1 colocalized with FM4-64 [*N*-(3-Triethylammoniumpropyl)-4-(6-(4-(Diethylamino)phenyl)hexatrienyl)Pyridinium Dibromide] along the PM (Fig. 3*A*). However, AFL1 was not evenly distributed along the PM and appeared in part as small foci along the membrane (*SI Appendix, Fig. S2F*). The strong interaction of AFL1 with AP2-2a (Fig. 2*A*), along with AFL1 localization, raised the possibility that AFL1 may be involved in trafficking of clathrin-coated vesicles (19). Consistent with this hypothesis, YFP-AFL1 colocalized with mOrange-labeled clathrin light chain (CLC) (25) at distinct foci along the PM (Fig. 3*B* and *SI Appendix, Fig. S10 A and B*). Foci of AFL1 often corresponded to small foci of CLC, indicative of the early stages of endocytotic vesicle formation (Fig. 3*B* and *C*). In other cases, AFL1–CLC colocalization could be seen at the junction between the CLC-labeled vesicle-like-particles and the PM (Fig. 3*B* and *C* and *SI Appendix, Fig. S10*). Internalized CLC-labeled structures detached from the PM had little or no colocalized AFL1. Likewise, AFL1 that was diffusely localized inside the cell did not colocalize with CLC (Fig. 3*B* and *C*). Occasionally, small puncta of colocalized AFL1 and CLC could be seen inside the cell, but this was less common. These patterns could be seen in both unstressed and stressed plants; however, AFL1–CLC colocalization (as measured by Pearson correlation coefficient, PCC) was significantly increased by stress (Fig. 3*D*). A range of PCC values was observed. In general, images that included many large internalized CLC-labeled vesicle-like structures had lower PCC values, whereas those with more CLC along the PM had higher PCC values (examples in *SI Appendix, Fig. S10B*). Bleed through between the YFP and mOrange channels was minimal (*SI Appendix, Fig. S10C*) and did not affect the results.

Tyrphostin A23, an inhibitor of clathrin-coated vesicle formation and endocytosis (14), blocked the increased proline accumulation of AFL1 O.E. plants but had no effect on *pdi5* or *nai2* mutants (Fig. 3*E*). This indicated that PDI5 and NAI2 affect proline accumulation by other mechanisms or act downstream of endocytosis. Tyrphostin A23 decreased the area of endosome-like particles decorated with AFL1 but had no substantial effect on AFL1 distribution along the PM or AFL1 protein levels (*SI Appendix, Fig. S11*). Internalization of AFL1 from PM was investigated using Brefeldin A (BFA). BFA resulted in some accumulation of YFP-AFL1 in BFA bodies, but this was not increased by stress, and the amount of AFL1 in BFA bodies was small compared with the amount along the PM (*SI Appendix, Fig. S12*). Together, the colocalization and BFA data indicated that AFL1 was associated with formation of clathrin-coated vesicles; however, AFL1 was not a major cargo protein internalized by clathrin-coated vesicles under stress.

Structural modeling using several publically available resources gave additional clues to AFL1 function. ModWeb found a similarity of AFL1 to a bacterial pore-forming toxin, amphiphysin, and moesin (*SI Appendix, Fig. S13*). Amphiphysin contains a Bin-Amphiphysin–reduced viability on starvation (BAR) domain that binds to sites of membrane curvature (26). I-Tasser found similarity to the same bacterial protein, as well as actinin, spectrin, another BAR domain protein (Atg17–Atg31–Atg29 complex), and cell adhesion components. Similarity to actin and clathrin binding sites was also found (*SI Appendix, Fig. S14*). The amphiphysin similarity is particularly interesting, as amphiphysin associates with AP2-2a at

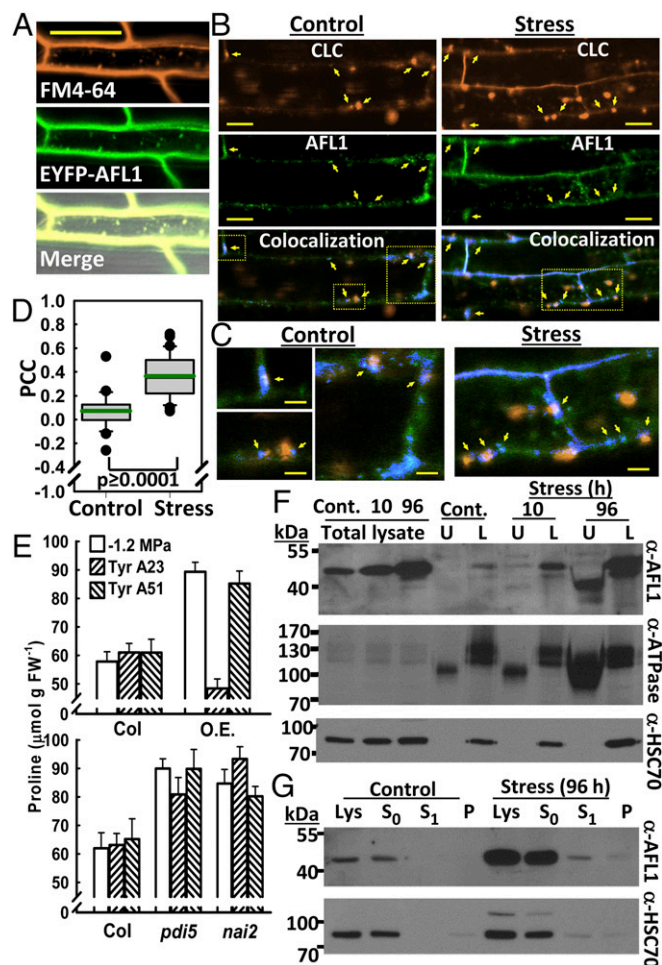


Fig. 3. AFL1 colocalization with CLC and membrane association. (A) Colocalization of FM4-64 and YFP-AFL1. Images are from representative root cells of seedlings transferred to -0.7 MPa for 96 h. (Scale bar, 50 μm .) (B) Colocalization of YFP-AFL1 with CLC-mOrange. Images are from representative root cells of control seedlings or after transfer to -0.7 MPa for 24 h. Yellow arrows indicate points of AFL1–CLC colocalization at putative sites of vesicle formation or at the margins of vesicle-like particles along the PM. (Scale bars, 20 μm .) (Bottom) (Colocalization) Blue indicates pixels with signal from both fluorophores. Yellow boxes in the colocalization panels indicate regions that are enlarged in C. (C) Sections of the colocalization images in B enlarged to show sites of AFL1–CLC colocalization at the margins of vesicle-like particles or at sites indicative of the early stages of vesicle formation (marked by arrows). (Scale bars, 5 μm .) (D) Quantification of YFP-AFL1 and CLC-mOrange colocalization by PCC. Boxes contain the 25th–75th percentiles of data points; whiskers indicate the 10–90 percentiles; outliers are shown as dots. Green line indicates the mean. $n = 24$ (control) and 43 (stress). (E) Proline accumulation in seedlings treated with Tyrphostin A23 or its negative analog A51 and transferred to -1.2 MPa for 96 h. *pdi5* and *nai2* indicate the combined data of *pdi5-1* and *pdi5-2* or *nai2-1* and *nai2-3*, respectively. O.E., AFL1 overexpression. Data are means \pm SE ($n = 12$) from two to three independent experiments. (F) Aqueous two-phase partitioning of membranes from seedlings under control conditions (Cont.) or exposed to stress (-1.2 MPa) for 10 or 96 h. L, lower phase fraction enriched for endomembranes; U, upper phase fraction enriched for PM. H^+ ATPase is a PM marker (the lower molecular weight bands) and HSC70 is an ER marker. Ten micrograms of protein per lane were loaded. (G) Detection of AFL1 in supernatant and membrane pellet after low salt extraction, followed by wash with normal buffer. Lys, total lysate; P, membrane pellet collected at the same time as the S₁ supernatant; S₀, supernatant after initial pelleting of membranes in low salt buffer; S₁, supernatant after wash with normal buffer. Forty micrograms of protein were loaded for each lane.

the neck of vesicles in the same complex as dynamin before the vesicle detaches from the PM (26). This agrees with our

observations of AFL1 interaction with AP2-2a and foci of AFL1 at and around sites of CLC concentration along the PM.

AFL1 Is a Peripheral Membrane Protein Associated with Both Plasma Membrane and Endomembranes. The structural modeling raised questions of whether AFL1 is really a transmembrane protein, as previously suggested for At14a (23, 24, 27, 28). Aqueous two-phase partitioning found that AFL1 associated with both PM and endomembrane (Fig. 3F). The localization was most clear after longer low ψ_w treatment, when AFL1 increased and could be seen in both membrane fractions. Similar results were observed for AFL1-FLAG O.E. plants (SI Appendix, Fig. S15). In this case, an increased amount of AFL1 in the lower fraction during stress, despite the constitutive expression, may indicate stabilization or altered turnover of AFL1. Interestingly, AFL1 was also detected in the supernatant during the initial stages of membrane fractionation (SI Appendix, Fig. S16A). Consideration of gel loading versus total volume of supernatant or membrane pellet indicated that most AFL1 was in the supernatant, rather than membrane pellet, and was of the higher molecular weight form (SI Appendix, Fig. S16A). Low salt (Fig. 3G) or EDTA (SI Appendix, Fig. S16 B and C) washes could completely remove AFL1 from the membrane pellet. Thus, AFL1 is membrane associated but not a transmembrane protein, similar to HSC70 (29).

AFL1 found in the endomembrane had higher-than-expected apparent molecular weight (the predicted molecular weight of AFL1 is 41.6 kDa), indicating that AFL1 may be posttranslationally modified. The nature of this posttranslational modification, and why it was present on the endomembrane-localized AFL1 but less detected in PM fractions, is not known. We also cannot rule out more complex patterns of AFL1 cleavage and modification. PDI5 or NAI2 could be involved in AFL1 posttranslational modification in the endomembrane system or control the trafficking of AFL1. However, fractionation of *pdi5-2*, *nai2-3*, and *pdi5-2nai2-3* found no substantial differences in AFL1 molecular weight distribution or total AFL1 protein amount compared with wild-type (SI Appendix, Fig. S17 A and B). These experiments do not rule out redundancy, for example, with other PDIs, which may obscure the role of PDI5 (or NAI2) in AFL1 modification.

Discussion

The strong effect of AFL1 on growth, gene expression, and proline accumulation demonstrated its role in drought resistance. AFL1 localization and protein interaction show it acts via mechanisms distinct from established drought-signaling pathways. The dramatic effect of AFL1 on drought response seems to be a combination of AFL1 function at the PM and endomembrane system (Fig. 4). Further parsing of which aspects of AFL1 function are most important for drought tolerance can now be pursued. We also found roles of PDI5 and NAI2 as negative regulators of growth and proline accumulation. For these reasons, as well as the novel structure of AFL1, our results offer a view of a previously unknown area of drought signaling.

At the PM, AFL1 was found in foci that colocalized with small foci of CLC indicative of the early stages of vesicle formation. In several cases, AFL1 was found at the intersection between CLC-labeled structures and the PM. These observations, as well as the interaction with AP2-2A, fit well with predicted similarity between AFL1 and BAR domain proteins, including amphiphysin. BAR domain proteins sense or induce membrane curvature (26). It can be readily hypothesized that membrane curvature is altered by loss of turgor, and AFL1 could be involved in responding to these membrane changes. Alternatively, AFL1 may promote vesicle formation in response to a stress-generated signal. AFL1 may also be present in larger complexes along the membrane, as suggested by its strong self-interaction in mbSUS assays and predicted similarity to spectrin.

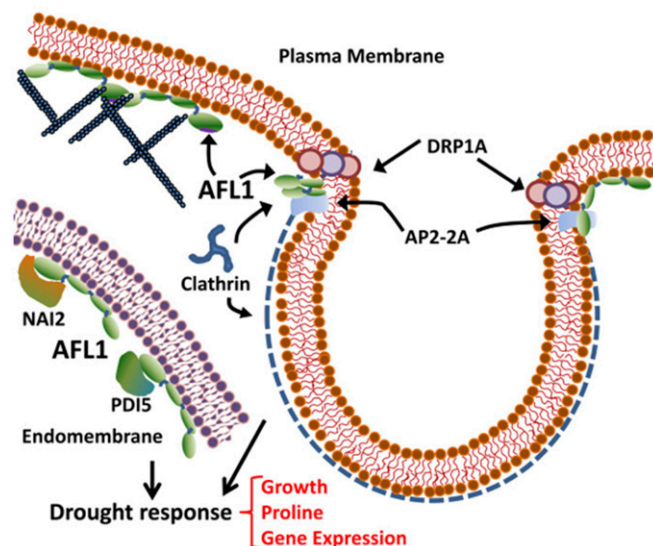


Fig. 4. Summary of AFL1 interactions and localization. AFL1 was found to be a peripheral membrane protein associated with both PM and endomembrane. At the PM, AFL1 interaction with AP2-2a and colocalization with CLC indicate a role in vesicle formation. Structural predictions also suggest AFL1 may interact with actin microfilaments. In endomembranes, AFL1 interacts with PDI5 and NAI2, which are negative effectors of drought response. In both membranes, AFL1 can also potentially interact with itself to form higher molecular weight complexes. Together, these roles of AFL1 have dramatic effect on drought response.

The structural predictions also indicated similarity of AFL1 to actinin, moesin, and vinculin, all of which are proteins associated with actin microfilaments. At14a has been proposed to affect cytoskeleton structure (23, 28), but the effect of this on stress response is unknown. Another possibility is that AFL1 association with the cytoskeleton is involved in generating force needed to deform the membrane in the early stages of vesicle formation. A number of cytoskeleton proteins were identified in AFL1 immunoprecipitates (Dataset S1), and testing whether AFL1 interacts directly with any of these will be a promising future direction. Overall, none of the proteins to which AFL1 has predicted similarity have clear orthologs in plants (30). It is possible that plants have combined these protein functions differently than mammalian cells to fit the unique structure of the plant PM and its interface with the cell wall, as well as the constraints turgor pressure can impose on vesicle formation and endocytosis.

In the endomembrane system, low ψ_w -stimulated interaction of AFL1 with PDI5 and NAI2 supports a specific function of these interactions in stress response. The similar AFL1 localization and molecular weight profile in *pdi5*, *nai2*, and *pdi5-2nai2-3* compared with wild-type suggest that PDI5 and NAI2 do not simply process AFL1 on its way to the PM (although redundancy among PDIs cannot be completely ruled out). Whether or not AFL1 affects PDI5 and NAI2 activity (or vice versa) is a question of interest. Physiologically, the observation that *pdi5-2nai2-3* had an even greater increase in growth than either single mutant indicates some overlap of PDI5 and NAI2 in drought response. However, PDI5 and NAI2 are not thought to have similar biochemical activities, and thus may affect (or be affected by) AFL1 differently. PDI5 is a regulator of protease activity (17), and the detection of several proteases as potential AFL1-regulated proteins (Fig. 1F, SI Appendix, Fig. S5, and Dataset S1) suggest that AFL1 may modify protease activity either directly or indirectly via PDI5.

Interestingly, our data indicate that AFL1 was present both in the ER lumen (where NAI2 and PDI5 are predominantly localized) and on the inner face of the PM (where colocalization

with CLC was observed). However, a protein that starts in the ER lumen and transits to the PM by exocytosis would be deposited on the outer face of the PM. A possible explanation for AFL1 on the inside of PM is that there are separate pools of AFL1, such that PM-associated AFL1 is synthesized in the cytosol and does not pass through the ER. It will also be of interest to consider whether the dual localization of AFL1 includes localization at sites of ER–PM contact, where exchange of information and materials between the two membrane systems could occur (15, 31).

The suppression of *RD21* [a procell death protease (32)] expression by AFL1 is consistent with recent examples that disabling negative regulators can enhance plant growth during drought or salt stress (1, 2, 33, 34). The idea that blocking cell death/senescence can promote growth under low ψ_w is in turn similar to results obtained using plants with drought-induced increases in cytokinin (35, 36). Indeed, this may be related to AFL1, as cytokinin metabolism and signaling genes were differentially expressed in AFL1 O.E. plants (Dataset S1), and a connection of At14a to cytokinin effect on Agrobacterium-mediated plant transformation was recently described (24).

AFL1-mediated enhancement of growth during drought raises the question of why AFL1 expression is not already higher in wild-type to promote growth. Likely, this represents a conservative strategy: continued leaf growth during drought can increase transpirational water loss beyond what can be supplied by the root system. Thus, even though growth could continue during moderate drought stress, it is actively down-regulated in anticipation of more severe stress. Perhaps more surprising is that root elongation is also subject to such negative regulation, despite numerous observations that root growth is relatively maintained under drought (37). Observation that AFL1 can circumvent this

negative regulation without inhibiting the growth of unstressed plants makes AFL1 a promising target for biotechnology.

Materials and Methods

Plant Material and Stress Treatment. Transgenic plants were prepared using vectors for expression of N-terminal YFP or C-terminal FLAG tagged AFL1 under control of the 35S promoter or DEX-induced RNAi suppression of AFL1. Stress treatments were performed by transferring seedlings to PEG-infused agar plates or by controlled soil drying (*SI Appendix, Materials and Methods*).

Protein Interaction. Immunoprecipitation of YFP-AFL1 was performed using GFP-trap beads (Chromtek) and proteins identified by liquid chromatography tandem mass spectrometry and database search. Yeast two-hybrid screening was performed using the ProQuest yeast two-hybrid system (Life Technologies), using a cDNA library constructed from seedlings treated at -1.2 MPa for 96 h. mbSUS assays were conducted using vectors, and yeast strains obtained from the *Arabidopsis* Biological Resource Center. BiFC assays and coimmunoprecipitation experiments were conducted using transient expression in intact *Arabidopsis* seedlings. Additional details are given in *SI Appendix, Materials and Methods*.

Subcellular Fractionation. Aqueous two-phase partitioning was performed (38) with minor modifications, as described in *SI Appendix, Materials and Methods*.

Microarray. Agilent microarrays were used for analysis of wild-type and AFL1 O.E. seedlings (*SI Appendix, Materials and Methods*), and the full data set was deposited (accession number GSE62413).

ACKNOWLEDGMENTS. We thank Sebastian Bednarek (University of Wisconsin–Madison) for the CLC-mOrange line; Christopher Grefen and Michael Blatt (University of Glasgow) for the rBiFC vectors; Mei-Jane Fang and Ji-Ying Huang for microscopy assistance; Choon-Kiat Lim, Thao T. Nguyen, and Trent Chang for laboratory assistance; Tuan-Nan Wen for proteomics analysis; and the Microarray Core Facility of the Institute of Plant and Microbial Biology for microarray processing. This work was supported by an Academia Sinica Career Development Award (to P.E.V.) and an Academia Sinica Postdoctoral Fellowship (to M.N.K.).

1. Claeys H, Inzé D (2013) The agony of choice: How plants balance growth and survival under water-limiting conditions. *Plant Physiol* 162(4):1768–1779.
2. Perrella G, et al. (2013) Histone deacetylase complex1 expression level titrates plant growth and abscisic acid sensitivity in Arabidopsis. *Plant Cell* 25(9):3491–3505.
3. Tardieu F, Parent B, Caldeira CF, Welcker C (2014) Genetic and physiological controls of growth under water deficit. *Plant Physiol* 164(4):1628–1635.
4. Baluska F, Samaj J, Wojtaszek P, Volkmann D, Menzel D (2003) Cytoskeleton-plasma membrane-cell wall continuum in plants. Emerging links revisited. *Plant Physiol* 133(2):482–491.
5. Monshausen GB, Gilroy S (2009) Feeling green: Mechanosensing in plants. *Trends Cell Biol* 19(5):228–235.
6. Monshausen GB, Haswell ES (2013) A force of nature: Molecular mechanisms of mechanoperception in plants. *J Exp Bot* 64(15):4663–4680.
7. Verslues PE, Bhaskara GB, Kesari R, Kumar MN (2014) Drought tolerance mechanisms and their molecular basis. *Plant Abiotic Stress*, eds Jenks MA, Hasagawa PM (Wiley Blackwell, Ames), 2nd Ed, pp 15–45.
8. Haswell ES, Verslues PE (2015) The ongoing search for the molecular basis of plant osmosensing. *J Gen Physiol* 145(5):389–394.
9. Christmann A, Grill E, Huang J (2013) Hydraulic signals in long-distance signaling. *Curr Opin Plant Biol* 16(3):293–300.
10. Shen H, Pirruccello M, De Camilli P (2012) SnapShot: Membrane curvature sensors and generators. *Cell* 150(6):1300.
11. Knepper C, Savory EA, Day B (2011) Arabidopsis NDR1 is an integrin-like protein with a role in fluid loss and plasma membrane-cell wall adhesion. *Plant Physiol* 156(1):286–300.
12. Nagpal P, Quatrano RS (1999) Isolation and characterization of a cDNA clone from *Arabidopsis thaliana* with partial sequence similarity to integrins. *Gene* 230(1):33–40.
13. Howell SH (2013) Endoplasmic reticulum stress responses in plants. *Annu Rev Plant Biol* 64:477–499.
14. Hachez C, et al. (2014) Arabidopsis SNAREs SYP61 and SYP121 coordinate the trafficking of plasma membrane aquaporin PIP2;7 to modulate the cell membrane water permeability. *Plant Cell* 26(7):3132–3147.
15. Perez-Sancho J, et al. (2015) The Arabidopsis synaptotagmin1 is enriched in endoplasmic reticulum-plasma membrane contact sites and confers cellular resistance to mechanical stresses. *Plant Physiol* 168(5):132–143.
16. Bhaskara GB, Nguyen TT, Verslues PE (2012) Unique drought resistance functions of the highly ABA-induced clade A protein phosphatase 2Cs. *Plant Physiol* 160(1):379–395.
17. Andème Ondzighi C, Christopher DA, Cho EJ, Chang SC, Staehelin LA (2008) Arabidopsis protein disulfide isomerase-5 inhibits cysteine proteases during trafficking to vacuoles before programmed cell death of the endothelium in developing seeds. *Plant Cell* 20(8):2205–2220.
18. Yamada K, Nagano AJ, Nishina M, Hara-Nishimura I, Nishimura M (2008) NAI2 is an endoplasmic reticulum body component that enables ER body formation in *Arabidopsis thaliana*. *Plant Cell* 20(9):2529–2540.
19. Fan L, et al. (2013) Dynamic analysis of Arabidopsis AP2 σ subunit reveals a key role in clathrin-mediated endocytosis and plant development. *Development* 140(18):3826–3837.
20. Grefen C, Blatt MR (2012) A 2in1 cloning system enables ratiometric bimolecular fluorescence complementation (rBiFC). *Biotechniques* 53(5):311–314.
21. Tsuda K, et al. (2012) An efficient Agrobacterium-mediated transient transformation of Arabidopsis. *Plant J* 69(4):713–719.
22. Nelson BK, Cai X, Nebenführ A (2007) A multicolored set of in vivo organelle markers for co-localization studies in Arabidopsis and other plants. *Plant J* 51(6):1126–1136.
23. Lü B, et al. (2012) AT14A mediates the cell wall-plasma membrane-cytoskeleton continuum in *Arabidopsis thaliana* cells. *J Exp Bot* 63(11):4061–4069.
24. Sardesai N, et al. (2013) Cytokinins secreted by Agrobacterium promote transformation by repressing a plant myb transcription factor. *Sci Signal* 6(302):ra100.
25. Konopka CA, Backues SK, Bednarek SY (2008) Dynamics of Arabidopsis dynamin-related protein 1C and a clathrin light chain at the plasma membrane. *Plant Cell* 20(5):1363–1380.
26. Daumke O, Roux A, Haucke V (2014) BAR domain scaffolds in dynamin-mediated membrane fission. *Cell* 156(5):882–892.
27. Lu B, Chen F, Gong ZH, Xie H, Liang JS (2007) Integrin-like protein is involved in the osmotic stress-induced abscisic acid biosynthesis in *Arabidopsis thaliana*. *J Integr Plant Biol* 49(4):540–549.
28. Lü B, et al. (2007) Intracellular localization of integrin-like protein and its roles in osmotic stress-induced abscisic acid biosynthesis in *Zea mays*. *Protoplasma* 232(1–2):35–43.
29. Arispe N, De Maio A (2000) ATP and ADP modulate a cation channel formed by Hsc70 in acidic phospholipid membranes. *J Biol Chem* 275(40):30839–30843.
30. Arabidopsis Genome Initiative (2000) Analysis of the genome sequence of the flowering plant *Arabidopsis thaliana*. *Nature* 408(6814):796–815.
31. Prinz WA (2014) Bridging the gap: Membrane contact sites in signaling, metabolism, and organelle dynamics. *J Cell Biol* 205(6):759–769.
32. Lampi N, Alkan N, Davydov O, Fluhr R (2013) Set-point control of RD21 protease activity by AtSerpin1 controls cell death in Arabidopsis. *Plant J* 74(3):498–510.
33. Dubois M, et al. (2013) Ethylene Response Factor6 acts as a central regulator of leaf growth under water-limiting conditions in Arabidopsis. *Plant Physiol* 162(1):319–332.
34. Skirycz A, et al. (2011) Survival and growth of Arabidopsis plants given limited water are not equal. *Nat Biotechnol* 29(3):212–214.
35. Rivero RM, et al. (2007) Delayed leaf senescence induces extreme drought tolerance in a flowering plant. *Proc Natl Acad Sci USA* 104(49):19631–19636.
36. Rivero RM, Shulaev V, Blumwald E (2009) Cytokinin-dependent photorespiration and the protection of photosynthesis during water deficit. *Plant Physiol* 150(3):1530–1540.
37. Sharp RE, et al. (2004) Root growth maintenance during water deficits: Physiology to functional genomics. *J Exp Bot* 55(407):2343–2351.
38. Larsson C, Widell S, Kjellbom P (1987) Preparation of high-purity plasma membranes. *Methods Enzymol* 148:558–568.